

# Speckle Noise and Soil Heterogeneities as Error Sources in a Bayesian Soil Moisture Retrieval Scheme for SAR Data

Matias Barber, *Student Member, IEEE*, Francisco Grings, Pablo Perna, Marcela Piscitelli, Martin Maas, Cintia Bruscantini, *Student Member, IEEE*, Julio Jacobo-Berlles, and Haydee Karszenbaum

**Abstract**—Soil moisture retrieval from SAR images is always affected by speckle noise and uncertainties associated to soil parameters, which impact negatively on the accuracy of soil moisture estimates. In this paper a soil moisture Bayesian estimator from polarimetric SAR images is proposed to address these issues. This estimator is based on a set of statistical distributions derived for the polarimetric soil backscattering coefficients, which naturally includes models for the soil scattering, the speckle and the soil spatial heterogeneity. As a natural advantage of the Bayesian approach, prior information about soil condition can be easily included, enhancing the performance of the retrieval. The Oh's model is used as scattering model, although it presents a limiting range of validity for the retrieval of soil moisture. After fully stating the mathematical modeling, numerical simulations are presented. First, traditional minimization-based retrieval is investigated. Then, it is compared with the Bayesian retrieval scheme. The results indicate that the Bayesian model enlarges the validity region of the minimization-based procedure. Moreover, as speckle effects are reduced by multilooking, Bayesian retrieval approaches the minimization-based retrieval. On the other hand, when speckle effects are large, an improvement in the accuracy of the retrieval is achieved by using a precise prior. The proposed algorithm can be applied to investigate which are the optimum parameters regarding multilooking process and prior information required to perform a precise retrieval in a given soil condition.

**Index Terms**—Bayesian methods, inverse problems, radar applications, soil moisture, synthetic aperture radar.

## I. INTRODUCTION

**S**URFACE soil moisture content plays a key role in the interaction between the land surface and the atmosphere, and accurate knowledge about this variable is of interest for a variety of reasons. First, it is strongly related to vegetation development. Second, it determines the partitioning between rainfall into infiltration and runoff, which is strongly related to erosion of top soil through leaching. Third, when soil moisture is high,

infiltration decreases and the risk of floods due to rainfall increases. And finally, soil evaporation and transpiration depends on soil moisture and therefore it influences the heat and mass transfers between the Earth and the atmosphere [1].

Following this demand of information, there is a systematic effort to develop maps of soil moisture of the Earth's surface. Orbiting microwave synthetic aperture radar (SAR) systems offer the opportunity of monitoring soil moisture content at different scales and under almost any weather condition, through the known sensitivity that the backscattered signal exhibits to soil parameters, including, among others, soil moisture and soil roughness [2]. Polarimetric SAR systems are able to transmit and receive radiation that is linearly polarized in the horizontal ( $h$ ) and vertical ( $v$ ) planes (relative to the plane defined by the wave vector and the normal to the surface being illuminated), giving rise to four intensity images  $\sigma_{hh}^0$ ,  $\sigma_{hv}^0$ ,  $\sigma_{vh}^0$ , and  $\sigma_{vv}^0$  of the target of interest [3].

However, the relation between backscattered signal and soil parameters is not straightforward, and consequently there are still no operational SAR-derived soil moisture products. There are two main reasons for this: (1) the scattering processes that relate backscattering to soil properties (moisture, roughness, and others) are difficult to model [4], and (2) the necessary input parameters are difficult to measure in the field [5], [6]. The former is mainly related to the SAR imaging system whereas the latter to soil parameters heterogeneity.

Moreover, usually there are several combinations of surface parameters producing the same SAR observations. As a consequence, any retrieving scheme is an ill-posed inverse problem. Accordingly, soil parameters retrieval remains challenging, and soil moisture products derived from remotely-sensed SAR data are still poorly accurate [7].

Restricting this study to bare soils, surface soil moisture presents a high degree of spatial variability at different scales, even for relatively small areas. This is associated to water-routing processes, radiative effects and heterogeneity in soil characteristics [5]. On the other hand, heterogeneity of surface roughness arises from both man-made and natural factors: tillage system, soil texture and soil type among others [6].

When using SAR images for retrieving soil properties, the speckle phenomenon, characteristic of SAR images, further hinders soil moisture retrieval. Speckle leads to a grain-like appearance of SAR images decreasing their contrast and radiometric

Manuscript received September 30, 2011; revised January 04, 2012; accepted March 07, 2012. Date of current version June 28, 2012. This work was supported by the Agencia Nacional de Promoción Científica y Tecnológica (ANPCyT) (PICT 1203) and MinCyT-CONAE-CONICET project 12.

M. Barber, F. Grings, P. Perna, M. Maas, C. Bruscantini, and H. Karszenbaum are with the Instituto de Astronomía y Física del Espacio (IAFE), Buenos Aires, Argentina (e-mail: mbarber@iafe.uba.ar).

M. Piscitelli is with the Cátedra de Conservación y Manejo de Suelos, Facultad de Agronomía, Universidad Nacional del Centro de la Pcia. de Buenos Aires (UNICEN), Buenos Aires, Argentina.

J. Jacobo-Berlles is with the Departamento de Computación, Facultad de Ciencias Exactas y Naturales (FCEN), Universidad de Buenos Aires (UBA), Buenos Aires, Argentina.

Digital Object Identifier 10.1109/JSTARS.2012.2191266

quality [3]. It is characteristic of the coherent nature of the SAR imaging system, can be modeled as a multiplicative noise and it is usually reduced in a post-processing stage by: (1) averaging neighboring pixels (multilooking process) at the expense of spatial resolution [8] or (2) using adaptive filters [9], to reduce radiometric uncertainties without losing spatial resolution, but at the expense of introducing artifacts. It is important to note that the process of averaging to reduce radiometric uncertainties implicitly assumes that soil properties within the average window are constant, which is usually not the case in most of the bare soils. Therefore, a trade-off between averaging and soil properties heterogeneity is usually accepted. However, heterogeneity of soil properties and speckle are usually considered as independent problems, whereas they are indeed a part of the same inference problem.

In this general framework, soil moisture retrieval over bare soils from SAR images can be considered an inference problem, where one essentially wants to infer soil condition given a set of measured backscatter coefficients and ancillary information. Polarimetric methods [10], [11], change detection procedures [12]–[14], possibilistic approaches [15], [16], radar backscatter modeling (theoretical and semi-empirical) [17]–[19], [4] and Bayesian approaches [20]–[22] are among the retrieval methodologies offered in the literature.

Polarimetric methods are based on modeling the backscatter response in terms of a certain polarimetric matrix decomposition (see [23] for a review) and taking into account the amplitude as well as the phase difference of the measured backscattering coefficients. Although polarimetry looks promising, a major effort is still needed to achieve an operational soil moisture retrieval algorithm using these techniques. Such algorithm was only developed in closed form for the Small Perturbation Model [11], which has a highly restrictive range of validity for the normalized RMS height ( $ks \ll 0.3$ , where  $k = 2\pi/\lambda$  is the wavenumber,  $\lambda$  the wavelength and  $s$  the RMS height), limiting operational soil parameter retrieval to very smooth surfaces. Therefore, this method is not suitable for real applications, where it is usually found values of  $ks \sim 0.3$  for L-band (i.e.,  $s = 1$  cm). In addition, speckle noise is not taken into account, although a polarimetric SAR speckle noise model was developed in [10].

Change detection methods exploit the availability of temporal series of SAR acquisitions from space platforms to monitor near-surface soil moisture content globally. The rationale behind this method is that temporal changes of surface roughness, canopy structure, and vegetation biomass occur over longer temporal scales than soil moisture changes, excluding periods of cultivation. Therefore, variations in surface backscatter observed with a short repeat cycle are expected to mainly reflect changes in soil moisture, since other parameters affecting radar backscatter can be considered fairly constant. Clearly, this sort of technique is constrained to spaceborne sensors with short-repeating cycles [12].

The possibilistic methods make use of an alternative set of axioms called fuzzy logic. As an advantage, they enable and require the use of prior information, which is used to improve

the retrieving of soil parameters. On the other hand, they do not take into account speckle and they are computationally intensive [15].

Regarding radar backscatter modeling approaches, a wide range of forward models, ranging from semi-empirical to theoretical, physically-based models have been developed in order to assess the dependency of soil parameters to backscattered signal. These models are important to understand the physics related to soil backscattering. They can also play a key role in the retrieval of soil condition from SAR measurements if an inverse problem approach is used [24], [25].

Physical Optics model (PO), Geometrical Optics model (GO), the first-order Small Perturbation Model (SPM) and the Integral Equation Model (IEM) [4] with its further improvements and updates [26]–[28] are the analytical electromagnetic backscattering models available. Their strength lies in the fact that they are derived from the well-established electromagnetic theory. However, the first three of them have been derived considering some specific assumptions and therefore have a limited applicability in terms of surface roughness. Although IEM is valid for a wider range of surface roughness conditions, the complexity of the model and the inherent relationship between soil parameters and soil backscattering make difficult to perform a direct retrieval.

Semi-empirical models are among the most popular for soil moisture retrieval applications. This is related to their simple algebraic formalism, that allows a straightforward retrieval scheme being the usual ones the direct inversion [18] and minimization (look-up table) procedures [19], [29]. The standard approach for the development of these models is to measure soil backscattering at different polarizations, incidence angles and soil conditions using scatterometers, for deriving a model by means of these measurements. In all the semi-empirical models available [17]–[19], only the mean value of the backscattering coefficient as a function of soil parameters is modeled, disregarding the spread around the average value and its causes. This gives rise to characteristic artifacts where several values of soil moisture estimated from scatterometer data correspond to the same soil moisture measured on the field [20]. Reasons for mismatches between model estimations and measured data include system measurement errors, the inhomogeneity of soil parameters within a given system resolution cell (or from one cell to the next) and the difficulty to measure soil parameters on the field [6], [30], [20]. Regarding this, the most difficult parameter to measure and to interpret is the surface correlation length [6]. Concerning the Oh's model [19], a simplified alternative version was modeled ignoring the correlation length, motivated by the insensitivity of the  $\sigma_{vh}^0 - \sigma_{vv}^0$  ratio on this roughness parameter.

To the authors' knowledge, it was not until Haddad *et al.* [20] that a systematic way to include uncertainties in a forward model based on Bayes' theorem was presented for the retrieval of soil parameters. The Bayesian framework has the relevant feature of naturally including many sources of uncertainty as well as many sources of information about the variables involved in the retrieval. Whereas the radar backscatter models

give rise to several combinations of surface parameters that map the same SAR observations, the Bayesian algorithm appropriately assimilates prior information on geophysical parameters in order to constrain the inversion of forward models. Despite these outstanding features, in their original paper Haddad *et al.* [20] only included as error source a term related to model uncertainties, and used only uniform distributions as prior. In addition, the potential of such Bayesian methodology is pointed out in [21] where data from active and passive sensors were merged in order to retrieve soil moisture. Nevertheless, up to date there is no model that incorporates multilooking speckle noise as an error source.

In this paper, we propose a Bayesian retrieval methodology which incorporates in a natural way soil parameters heterogeneity and speckle as sources of uncertainty that degrade the estimated soil moisture. Such a Bayesian approach (1) needs only a forward model, (2) gives the optimal estimator for the soil moisture and its error, (3) can include as many error sources as required and (4) can include prior information in a systematic way. The methodology will be presented using a simplified version of the Oh's model [19] as the forward model.

The present paper has been divided as follows. In Section II a brief description of the general properties of scatterometer-based semi-empirical forward models is presented, focused on Oh's model and the multiplicative model. Section III is devoted to present the statistical model, and Bayesian estimators are derived. Numerical results are reported in Section IV. Finally, Section V presents the main conclusions derived from this study.

## II. SCATTEROMETER-BASED SEMI-EMPIRICAL FORWARD MODELS

### A. Oh's Model

One of the most widely used semi-empirical soil scattering models is the one developed by Oh [19], where model expressions are physically-based, but model parameters are fitted using data from an extensive database of polarimetric radar scatterometer measurements over bare soils. In its simplified version, where the correlation length is disregarded, the Oh's model relates backscattering coefficients and certain bare soil properties through a set of three analytical functions  $\sigma_i^0$ , that can be symbolically expressed as [19, eqs. (1),(2) and (4)],

$$x_i = \sigma_i^0(m, ks) \quad (i = 1, 2, 3), \quad (1)$$

where  $x_i$  is the backscattering (measured) coefficients and the subscript  $i = 1, 2, 3$  stands respectively for the  $hh$ -,  $vv$ - and  $vh$ -polarizations. The backscattering coefficients  $x_i$  are functionally related to the volumetric soil moisture content  $m$  ( $\text{cm}^3/\text{cm}^3$ ) and the normalized surface soil RMS height  $ks$  (where  $k = 2\pi/\lambda$  is the wavenumber and  $s$  the RMS height) throughout the functions  $\sigma_i^0$ . This model also depends on the system incidence angle  $\theta$ , which is a known parameter. Throughout this paper, it will be assumed that  $\theta = 35^\circ$ . The Oh's model is constrained to the range  $0.04 \leq m \leq 0.291$  and

$0.13 \leq ks \leq 6.98$ , although a better agreement between the model and the experimental results is obtained for  $ks \leq 3.5$  [19]. Explicitly from [19, eqs. (1),(2) and (4)],

$$\sigma_{vh}^0 = 0.11m^{0.7}(\cos\theta)^{2.2}[1 - \exp(-0.32(ks)^{1.8})], \quad (2)$$

$$\sigma_{vv}^0 = \frac{\sigma_{vh}^0(m, ks)}{0.095(0.13 + \sin(1.5\theta)^{1.4}[1 - \exp(-1.3(ks)^{0.9})]}, \quad (3)$$

$$\sigma_{hh}^0 = \sigma_{vv}^0(m, ks) \left[ 1 - \left( \frac{\theta}{90^\circ} \right)^{0.35m^{-0.65}} \exp(-0.4(ks)^{1.4}) \right]. \quad (4)$$

Concerning the  $\sigma_i^0$  functions, it is worth mentioning that they are not independent of each other, since by (1) there are three equations and only two variables. Then, providing that  $m$  and  $ks$  are given, it always holds

$$\sigma_{hh}^0 = \tilde{f}_1(m, ks)\sigma_{vv}^0 \quad (5)$$

$$\sigma_{vh}^0 = \tilde{f}_3(m, ks)\sigma_{vv}^0, \quad (6)$$

thus indicating that both  $hh$  and  $vh$  backscattering coefficients are a rescaled version of  $vv$ , where the derivation of functions  $\tilde{f}_1$  and  $\tilde{f}_3$  is straightforward from (4) and (3), respectively. This is a consequence of the deterministic nature of the Oh's model. From (2), (3) and (4), it is easy to show that the backscattering coefficients for  $\sigma_{hh}^0$ ,  $\sigma_{vv}^0$  and  $\sigma_{vh}^0$  increase monotonically with  $m$  and  $ks$ , but with different slopes in each variable; for a bare soil,  $\sigma_{vv}^0$  is always greater than  $\sigma_{hh}^0$  and the latter greater than  $\sigma_{vh}^0$ . Any retrieval scheme using Oh's model is based on the differential sensitivity exhibited by the backscattering coefficients to  $m$  and  $ks$ . The dynamic range in dB of the backscattering coefficients ((2)–(4)) is given in a nested way from the simplified formulation of the Oh's model, constrained to  $ks \leq 3.5$  and for  $\theta = 35^\circ$ :

$$-42.2 \text{ dB} < \sigma_{vh}^0 < -15.6 \text{ dB}, \quad (7)$$

$$\sigma_{vh}^0 + 10.8 \text{ dB} < \sigma_{vv}^0 < \sigma_{vh}^0 + 18.0 \text{ dB} \quad (8)$$

and

$$\sigma_{vv}^0 - 2.7 \text{ dB} < \sigma_{hh}^0 < \sigma_{vv}^0. \quad (9)$$

The inequations (7), (8) and (9) define a region where Oh's model is valid (Oh's model validity region). Only points  $(\sigma_{hh}^0, \sigma_{vv}^0, \sigma_{vh}^0)$  within this region may be used to retrieve  $(m, ks)$  using Oh's model.

Considering the aim of this work, differences between the backscattering coefficients measured from SAR systems and the ones measured from ground-based scatterometers have to be analyzed. First, the ground-based scatterometer footprint is small; the actual size varies for different experiments and sensors, but it is always of the order of a few squared meters. This is justified assuming that the soil properties on which measured microwave backscattering depends (soil moisture and roughness) are constant inside the sampled area. Therefore, it is reasonable to assume that the backscattering coefficient of the study area is a function of a single soil moisture value and roughness profile. In other words, the terrain scattering properties within the footprint can be considered constant. Second, it is easy to average

several measurements upon the same surface's target and thus reduce the speckle noise.

On the other hand, SAR system resolution is larger (of the order of hundreds of  $m^2$ ) and even larger if we want to average and increase the number of looks to reduce speckle. Therefore, any retrieval scheme based on SAR data that uses scatterometer-based models should deal with the heterogeneity of soil properties and speckle. This will lead to non-constant soil scattering properties in the averaging window and/or non-negligible speckle noise, which in any case will degrade soil moisture retrieval.

### B. Multiplicative Model

The multiplicative model is generally used to model the SAR response of a target as a function of the combined effect of terrain backscattering and speckle noise. Specifically, the model states that the observed intensity value in every pixel of a SAR image is the outcome of a random variable  $Z$ , called return, defined as the product between the random variables  $X$  and  $Y$ , where  $X$  represents the random variable modeling the variations of terrain backscattering properties and  $Y$  represents the random variable modeling the speckle noise; i.e.,  $Z = XY$  [3].

Different probability density distributions (PDF) for  $X$  and for  $Y$  yield different models for the observed data  $Z$ . For homogeneous regions, the terrain scattering properties are assumed constant. Therefore, the distribution of  $Z$  is a rescaled version of the distribution of  $Y$ , which is usually assumed as Gamma-distributed with parameters  $(n, n)$  and mean value  $E[Y] = 1$  [3],

$$P_Y(y) = \frac{n^n}{\Gamma(n)} y^{n-1} e^{-ny} \quad (10)$$

where  $n$  is the equivalent number of looks and  $\Gamma(n)$  is the Gamma function. Since  $Var[Y] = 1/n$ , as  $n$  approaches to infinity, the radiometric uncertainty becomes negligible.

The basic hypothesis that governs the modeling of inhomogeneous regions ( $X \neq constant$ ) is that they can be modeled by a convenient distribution. In our case, we will propose a PDF for  $X$  that arises as the result of inter-pixel soil parameters heterogeneity. Indeed, if soil parameters changes from pixel to pixel, soil backscattering (which is a function of soil parameters) will also change accordingly. In order to account for backscattering variability arising from soil parameters heterogeneity, we will derive the corresponding PDF using Oh's model, for all the polarizations.

By means of the multiplicative model, we can include two independent sources of SAR image inhomogeneity: soil spatial variability and speckle. This idea can be formalized as follows. First, we will assume that  $X$  and  $Y$  are independent. Second, that the average properties of the return  $Z$  will be determined by the average properties of both  $X$  and  $Y$ , since by virtue of the multiplicative model,

$$E[Z] = E[X]E[Y]. \quad (11)$$

Suitable distributions for  $X$  and  $Y$  will be introduced in Sections III-C and III-D.

## III. STATISTICAL MODEL

### A. Bayesian Approach

The deterministic forward model developed by Oh can be extended to a stochastic model following [20]. In doing so, we can include in the forward model both the terrain heterogeneity and speckle through the multiplicative model,

$$Z_i = X_i Y_i \quad (i = 1, 2, 3), \quad (12)$$

where  $Z_i$  is the random variable which represents the return  $z_i$  and the subscript  $i$  stands for the different polarizations, as stated before.  $X_i$  and  $Y_i$  are independent random variables that model the heterogeneity of the target backscattering and the speckle noise, respectively.

We assumed that the target response to the backscatter is modeled through the Oh's model by  $X_i = \sigma_i^0(M, KS)$  ( $i = 1, 2, 3$ ), where the  $\sigma_i^0$  are the same as in (1) and represent here the deterministic way in which the random variable  $X$  depends on the random variables  $M$  and  $KS$  (which represent the  $m$ 's and  $ks$ 's of the target). In other words, an heterogeneous soil will produce a wide range of possible outcomes  $x$  of  $X$ , provided a wide range of soil moisture and roughness values were presented in the soil. On the other hand, an extremely homogeneous soil (i.e., a certain mean value  $(\bar{m}, \bar{ks})$  with a very low variance) will produce a very narrow probability density function for  $X$ . This statement is mathematically grounded by means of a Taylor expansion, namely  $E[X_i] = E[\sigma_i^0(M, KS)] = \sigma_i^0(\bar{m}, \bar{ks}) + O(Var(M), Var(KS))$ , where  $\bar{m}$  and  $\bar{ks}$  are the expected or mean values of  $M$  and  $KS$  within the resolution cell and higher order terms are neglected. Therefore,  $E[X_i] \approx \sigma_i^0(\bar{m}, \bar{ks})$  as long as the variance remains low, for all  $i = 1, 2, 3$ . In addition, following [3] the speckle adds only a multiplicative noise so that  $E[Y_i] = 1$  ( $i = 1, 2, 3$ ). This approach leads into a proper average behavior for the returns  $Z_i$  in terms of the forward Oh's model since  $E[Z_i] = \sigma_i^0(\bar{m}, \bar{ks})$  under the assumption of independence of  $X$  and  $Y$ .

From the set of (12) and using Bayes' theorem, an expression for the conditional ("posterior") probability of measuring  $m$  and  $ks$  given measurements of returns  $z_1, z_2$  and  $z_3$  can be obtained,

$$P(m, ks | z_1, z_2, z_3) = \frac{P_{Z_1 Z_2 Z_3}(z_1, z_2, z_3 | m, ks) P_{MK S}(m, ks)}{P_{Z_1 Z_2 Z_3}(z_1, z_2, z_3)}, \quad (13)$$

where  $P_{Z_1 Z_2 Z_3}(z_1, z_2, z_3 | m, ks)$  is the probability of measuring a certain set  $(z_1, z_2, z_3)$  of returns given measurements of  $m$  and  $ks$  (the "likelihood"),  $P_{MK S}$  is the prior joint density function of  $m$  and  $ks$  (where it is included all the prior information about  $m$  and  $ks$ ) and  $P(z_1, z_2, z_3)$  works as a normalizing factor and it is the probability of a certain set  $(z_1, z_2, z_3)$  to be measured. Then, providing the conditional density function (13) is exact, the optimal unbiased estimator of  $m$  that has the minimum variance is the mean of (13) [31],

$$m_{est}^{Bayes} = \int \int_D m P(m, ks | z_1, z_2, z_3) dm dks \quad (14)$$

and similarly the squared standard deviation of this estimator will be:

$$m_{std}^2 = \int \int_D (m - m_{est}^{Bayes})^2 P(m, ks | z_1, z_2, z_3) dm dks \quad (15)$$

where an explicit expression for (13) must be found in order to calculate  $m_{est}^{Bayes}$  and  $m_{std}$ . The integration domain  $D$  in (14) and (15) spans the same range of  $(m, ks)$  where the forward Oh's model was originally constrained, except for  $ks$  which is taken to be  $\leq 3.5$  as discussed in Section II-A. The standard deviation  $m_{std}$  can be used as a measure of the error of the estimate  $m_{est}^{Bayes}$ .

### B. Derivation of the Likelihood

The posterior distribution  $P(m, ks | z_1, z_2, z_3)$  in (13) can be computed as follows. First, using recursively the definition of conditional probability yields

$$P_{Z_1 Z_2 Z_3}(z_1, z_2, z_3 | m, ks) = P_{Z_1}(z_1) P_{Z_2 | Z_1=z_1}(z_2) \times P_{Z_3 | Z_1=z_1, Z_2=z_2}(z_3) \quad (16)$$

where in the right term the given  $m$  and  $ks$  were suppressed for simplicity. In (16),  $P_{Z_1}(z_1)$  is calculated using the change of variables theorem upon (12) ( $i = 1$ ) and the assumption of independence between  $X$  and  $Y$ ,

$$P_{Z_1}(z_1) = \int_0^\infty P_{X_1}(w) P_{Y_1}\left(\frac{z_1}{w}\right) \frac{1}{w} dw. \quad (17)$$

In order to calculate the remaining two terms in (16), it might be noted that replacing  $m$  by  $M$  and  $ks$  for  $KS$  in (5) and (6) the following relationships concerning  $X_i$  hold

$$X_1 = \tilde{f}_1(M, KS) X_2 \quad (18)$$

$$X_3 = \tilde{f}_3(M, KS) X_2. \quad (19)$$

Replacing this set of equation in (12) and then equating for  $Z_2$  and  $Z_3$  one obtains

$$Z_2 = \frac{1}{\tilde{f}_1(M, KS)} \frac{Y_2}{Y_1} Z_1 \quad (20)$$

$$Z_3 = \tilde{f}_3(M, KS) \frac{Y_3}{Y_2} Z_2. \quad (21)$$

Finally, given  $m$  and  $ks$  and using again the change of variables theorem upon (20) and (21) separately, the remaining conditional probabilities are

$$P_{Z_2 | Z_1=z_1}(z_2 | m, ks) = \frac{\tilde{f}_1(m, ks)}{z_1} P_{Y_2/Y_1} \left( \frac{\tilde{f}_1(m, ks) z_2}{z_1} \right), \quad (22)$$

$$P_{Z_3 | Z_1=z_1, Z_2=z_2}(z_3 | m, ks) = \frac{1}{\tilde{f}_3(m, ks) z_2} P_{Y_3/Y_2} \left( \frac{z_3}{\tilde{f}_3(m, ks) z_2} \right), \quad (23)$$

where  $P_{Y_i/Y_j}$  ( $i \neq j$ ) is the joint distribution of the ratio of two multilooked random variables that are affected by speckle. The

likelihood in (16) is constructed then by multiplying (17), (22) and (23).

### C. Modeling the Terrain Backscatter $X$

Natural variability of soil moisture are always present at different scales, and thus also at the scale of SAR systems [32]. In general, this implies that soil moisture inside a field cannot be considered constant; i.e., the field is heterogeneous in terms of soil moisture. Soil roughness can also be framed within this description. In agricultural fields, roughness is generated artificially by tilling and naturally by wind and water erosion. Moreover, soil surface roughness is very dependent on soil type [33].

In order to define the PDF of  $X$  arising from randomness in  $M$  and  $KS$ , a forward model is needed. It is important to remark that errors introduced by the forward model set a lower bound of uncertainty in any retrieval scheme. In the approach developed in this paper, forward model uncertainties were not considered, because the focus is placed on addressing the relative contribution of prior information and multilooking process on the retrieval errors.

This mapping will be completely defined by the functions  $\sigma_i^0$  from (1) that associate soil backscattering with soil parameters (i.e., the forward model). To compute this mapping, we will use a three-step procedure given in [34, §2.12]. Such a procedure allows to find the distribution  $P_R$  of a general function  $r(u, v)$  which depends on two random variables  $U$  and  $V$  of known distribution. In our case, we are interested on the computation of the distribution of  $x_1 = \sigma_{hh}^0(m, ks)$  used in (17) as  $P_{X_1}$  when the soil moisture  $m$  and roughness  $ks$  are considered random variables  $M$  and  $KS$ , respectively. Ignoring the subscript 1, such computation states that

$$F_X(x) = \int \int_{A_x} P_{MKS}(m, ks) dm dks, \quad (24)$$

where  $F_X(x)$  is the cumulative distribution function of the random variable  $X$  and the integration domain is  $A_x = \{(m, ks) : \sigma_{hh}^0(m, ks) \leq x\}$ . Then  $P_X(x)$  is readily obtained by deriving (24) with respect to  $x$ . In what follows, it would be assumed that  $M$  and  $KS$  are uncorrelated and Gaussian random variables, so that  $P_{MKS} = P_M P_{KS}$  where  $P_M \sim N(\bar{m}, \sigma_m)$  and  $P_{KS} \sim N(\bar{ks}, \sigma_{ks})$ . Therefore, the heterogeneity of the soil parameters within a SAR pixel is controlled throughout the variance  $\sigma_m^2$  and  $\sigma_{ks}^2$ . The Gaussian assumption is not restricting or fundamental in any way, and the procedure can be also applied to different distributions for  $m$  and  $ks$ , even empirical ones. On the other hand, under this assumption the computation of (24) can be only performed numerically.

### D. Modeling the Speckle Noise $Y$

Statistical properties of multilook polarimetric data are quite different from those of single-look data [8]. Therefore, in order to model the expected speckle phenomena, we need to know the probability density function of polarimetric data as a function of the number of looks  $n$ . In the case of multilook intensity values, the corresponding distribution  $P_Y$  is that of (10) and is used in

(17). On the other hand, the probability density function of the ratio of two multilook polarimetric data sets  $P_{Y_i/Y_j}$  which are not independent is required in (22) and (23). Such a distribution was derived by Lee *et al.* [8]:

$$P_U(u) = \frac{\Gamma(2n)}{\Gamma(n)\Gamma(n)} \frac{\tau^n (1 - |\rho_u|^2)^n (\tau + u) u^{n-1}}{[(\tau + u)^2 - 4\tau|\rho_u|^2 u]^{n+1/2}} \quad (25)$$

where  $U = Y_i/Y_j$  ( $i \neq j$ ),  $n$  is the number of looks,  $\rho_c$  is the correlation between the numerator and the denominator and  $\tau = E[Y_i]/E[Y_j]$  is the ratio of the expected value of  $Y_i$  and  $Y_j$ . In order to determine the expected value of the returns only by the expected value of the forward model, we stated that  $E[Y_i] = 1$  ( $i = 1, 2, 3$ ) and then  $\tau = 1$ . Thus the expected value of  $Z$  is determined only by  $X$  as follows from (11). The ratio distribution also depends on the correlation between the numerator and the denominator  $\rho_u$ . This is very important, since when numerator/denominator correlation increases, the variance of the distribution decreases [8]. As expected, when  $n$  increases the distribution becomes narrower and thus the variance of the estimates decreases, leading to a more precise retrieval. Up to this point, we presented all the mathematics needed in a Bayesian retrieval scheme. In the next sections we present the results of numerical simulations.

#### IV. NUMERICAL RESULTS

##### A. Minimization Estimate

Since Oh's model is not directly invertible, in [19] it is presented an algorithm for retrieving soil moisture and roughness from a set of measured backscattering coefficients  $\sigma_{hh}^0$ ,  $\sigma_{vv}^0$  and  $\sigma_{vh}^0$  through a minimization procedure. Such a procedure is based on the simultaneous solution of model (2), (3) and (4), leading to the following non-linear expression [19, eq. (6)],

$$1 - \left( \frac{\theta}{90^\circ} \right)^{0.35m^{-0.65}} \exp(-0.4(ks(\theta, m, \sigma_{vh}^0))^{1.4}) - \frac{\sigma_{hh}^0}{\sigma_{vv}^0} = 0 \quad (26)$$

where  $ks(\theta, m, \sigma_{vh}^0)$  is directly obtained after solving (2). For a given  $(\sigma_{hh}^0, \sigma_{vv}^0, \sigma_{vh}^0)$ , the estimated value of  $m$  is the one that minimizes this expression, namely  $m_{est}^{Oh}$ . It is important to note that (26) can be solved only for the values of  $(\sigma_{hh}^0, \sigma_{vv}^0, \sigma_{vh}^0)$  that are allowed by the forward model, specifically those values that lie within the region bounded by inequations (7), (8) and (9). This means that this approach is not robust to high statistical fluctuations in the backscattering coefficients, that are commonly found in real applications.

Assuming a certain value for  $\sigma_{vh}^0$  ( $\sigma_{vh}^0 = -25$  dB) and  $\theta = 35^\circ$ , when applying to the entire  $(\sigma_{hh}^0, \sigma_{vv}^0)$ -space a root-finding procedure applied on (26) gives rise to the contour lines depicted on Fig. 1. Although the levels of the contour lines span the entire range of Oh's model (0.04 – 0.291  $\text{cm}^3/\text{cm}^3$ ), only the levels corresponding to 0.05, 0.10, 0.15, 0.20 and 0.25 (in units of  $\text{cm}^3/\text{cm}^3$ ) are drawn. The linear trend of the contour lines is consistent with the fact that at fixed  $vh$ , the dynamical range of the minimization estimates from (26) is governed by the ratio  $\sigma_{hh}^0/\sigma_{vv}^0$ , which takes constant values over lines in the entire  $(\sigma_{hh}^0, \sigma_{vv}^0)$ -space. To corroborate the inversion, the

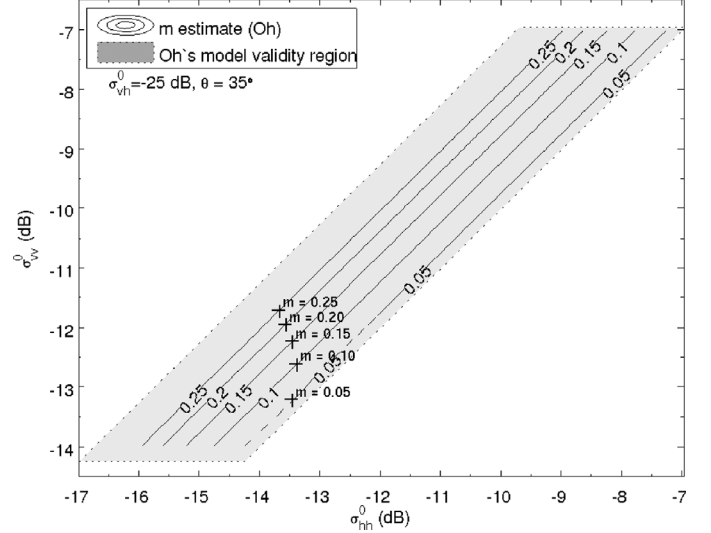


Fig. 1. Soil moisture  $m_{est}^{Oh}$  estimated on the  $(\sigma_{hh}^0, \sigma_{vv}^0)$ -plane (at fixed  $\sigma_{vh}^0 = -25$  dB) from Oh's model, in units of  $\text{cm}^3/\text{cm}^3$ . The light gray area encloses the pairs  $(\sigma_{hh}^0, \sigma_{vv}^0)$  where the model is valid.

exact values of  $m$  were computed using the deterministic forward Oh's model (1), constrained to the assumption that  $\sigma_{vh}^0 = -25$  dB ('+' marks in Fig. 1). The levels of the exact values agree with those of the minimization estimates.

Every value of  $(\sigma_{hh}^0, \sigma_{vv}^0, \sigma_{vh}^0)$  yields in a value of  $m_{est}^{Oh}$  inside Oh's model validity region, as expected, whereas for the values of  $(\sigma_{hh}^0, \sigma_{vv}^0, \sigma_{vh}^0)$  lying outside that region the inversion technique cannot produce a retrieval. The latter situation could be related to shortcomings of the forward model, landcover uncertainties (i.e., the target is not completely bare soil), speckle noise and/or system fluctuations. In an operational implementation, the spurious estimations related to the landcover can be reduced using ancillary information about landcover status. Nevertheless, it is important to remark that even bare soil can produce values of  $(\sigma_{hh}^0, \sigma_{vv}^0, \sigma_{vh}^0)$  outside the Oh's model validity region, due to speckle and system fluctuations.

The estimation procedure from (26) produces a single value of  $m_{est}^{Oh}$  given a set of measured values  $(\sigma_{hh}^0, \sigma_{vv}^0, \sigma_{vh}^0)$ . No ancillary information about soil status (previous or estimated by other means) is allowed. Moreover, it is implicitly assumed that image radiometric uncertainties are very low, since small fluctuation of measured values can produce strong variations in soil moisture estimation. Therefore, in order to successfully use this type of retrieval, a speckle reduction technique is mandatory.

##### B. Bayesian Estimate

An alternative method for the estimation of  $m$ , which is suitable for taking into account the speckle, arises when using the expressions (14) and (15). In order to test the goodness of the Bayesian approach, a uniform prior is used as  $P_{MKS}$  in (13). This kind of prior represents the lack of knowledge about soil condition. Specifically, it is taken  $P_M \sim U(0.04, 0.35)$  and  $P_{KS} \sim U(0.13, 3.5)$  as reasonable priors, covering the range of Oh's model.

Fig. 2 shows a contour plot of the estimate  $m_{est}^{Bayes}$  for soil moisture, as a function of the measured values of  $\sigma_{hh}^0$

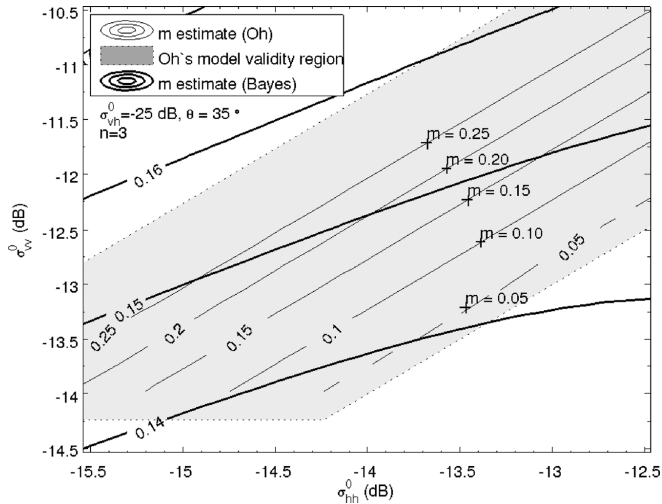


Fig. 2. Comparison between the soil moisture estimated using Oh's model and the Bayesian retrieval approach, in units of  $\text{cm}^3/\text{cm}^3$ . The parameters adopted by the simulation are:  $n = 3$ ,  $\sigma_m = 0.005 \text{ cm}^3/\text{cm}^3$ ,  $\sigma_{ks} = 0.01$ ,  $\rho_{\sigma_{vv}^0/\sigma_{hh}^0} = 0.7$  and  $\rho_{\sigma_{vh}^0/\sigma_{vv}^0} = 0.1$ .

and  $\sigma_{vv}^0$  with  $n = 3$ , for  $\sigma_{vh}^0 = -25 \text{ dB}$  and  $\theta = 35^\circ$ . The light shaded area represents Oh's model validity region, where the contour lines of soil moisture derived from the Oh's model are also shown. The remaining model parameters are  $\sigma_m = 0.005 \text{ cm}^3/\text{cm}^3$ ,  $\sigma_{ks} = 0.01$ ,  $\rho_{\sigma_{vv}^0/\sigma_{hh}^0} = 0.7$  and  $\rho_{\sigma_{vh}^0/\sigma_{vv}^0} = 0.1$ . When using the Bayesian methodology, the retrieved soil moisture values cover the entire  $(\sigma_{hh}^0, \sigma_{vv}^0, \sigma_{vh}^0)$ -space, although the extreme values (the ones that are far away from Oh's model validity region (shaded area)) will present a very low probability of occurrence associated. The high spread shown by the contour lines is consistent with the high variance of the speckle noise for this small number of looks ( $n = 3$ ).

In Fig. 2 the results of both estimations (minimization and Bayesian) are compared. It is readily seen that  $m_{est}^{Oh}$  and  $m_{est}^{Bayes}$  do not coincide. Since the prior is uniform, this discrepancy is related to the chosen values of model parameters  $\sigma_m$ ,  $\sigma_{ks}$  and  $n$ . The choice of  $\sigma_m = 0.005 \text{ cm}^3/\text{cm}^3$ ,  $\sigma_{ks} = 0.01$  corresponds to a very homogeneous soil, which corresponds to low variance is the soil backscattering  $X$ . However,  $n = 3$  corresponds to a high variance in the speckle  $Y$ , which ultimate leads to a poor soil moisture estimation. This statement is reflected in the contour lines of one-sigma standard deviation of  $m_{est}^{Bayes}$  depicted on Fig. 3 and calculated by means of (15). The standard deviation reaches a relative high value (about 2/5 of the dynamic range for soil moisture) of  $\sim 0.07 \text{ cm}^3/\text{cm}^3$  in everywhere.

Fig. 4 shows the contour lines retrieved after increasing the number of looks to  $n = 256$ . When significant multilooking is present, the Bayesian retrieval looks more compact around the contour lines of Oh's model indicating, to some extent, a correct asymptotical behavior. It could be seen that the '+' marks and the Bayes' contour lines agree, especially for the levels of 0.10, 0.15 and 0.20 in units of  $\text{cm}^3/\text{cm}^3$ . Of course, since the minimization and Bayesian estimators are different, an overlap of the contour lines is not expected. In the same way, Fig. 5 depicts the contour lines of one-sigma standard deviation of  $m_{est}^{Bayes}$  calculated by means of (15) for  $n = 256$ . In this case, the standard

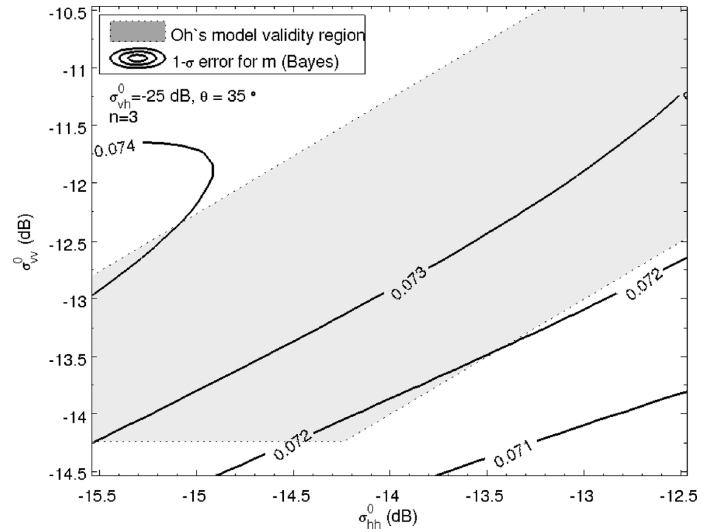


Fig. 3. One-sigma standard deviation of  $m_{est}^{Bayes}$  for a number of looks  $n = 3$ , in units of  $\text{cm}^3/\text{cm}^3$ . The parameters adopted by the simulation are:  $\sigma_m = 0.005 \text{ cm}^3/\text{cm}^3$ ,  $\sigma_{ks} = 0.01$ ,  $\rho_{\sigma_{vv}^0/\sigma_{hh}^0} = 0.7$  and  $\rho_{\sigma_{vh}^0/\sigma_{vv}^0} = 0.1$ .

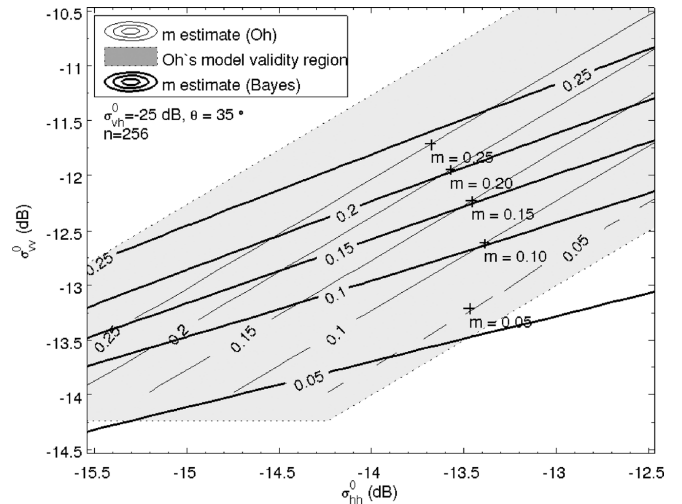


Fig. 4. Comparison between the soil moisture estimated using Oh's model and the Bayesian retrieval approach, in units of  $\text{cm}^3/\text{cm}^3$ . The parameters adopted by the simulation are:  $n = 256$ ,  $\sigma_m = 0.005 \text{ cm}^3/\text{cm}^3$ ,  $\sigma_{ks} = 0.01$ ,  $\rho_{\sigma_{vv}^0/\sigma_{hh}^0} = 0.7$  and  $\rho_{\sigma_{vh}^0/\sigma_{vv}^0} = 0.1$ .

deviation ranges between a minimum of  $\sim 0.005 \text{ cm}^3/\text{cm}^3$  and reaches a maximum value of  $\sim 0.03 \text{ cm}^3/\text{cm}^3$ . The relative improvement in the case shown in Fig. 3 is due to the increasing number of looks, which is a way to reduce the uncertainties due speckle in soil moisture estimation.

### C. Including Prior Information

If prior information is on hand, the Bayesian retrieval scheme can include it straightforwardly. Prior information can be available from historical records, estimations from other sensors, in situ data and/or contextual information about soil texture/use. Using this information, suitable distributions for the prior distributions of soil moisture and roughness can be estimated.

As an example, we now assumed that the prior distribution for soil roughness in the study area is Gaussian distributed

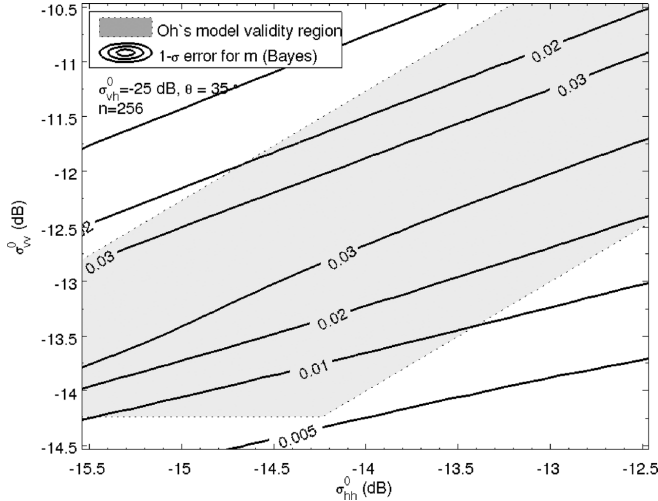


Fig. 5. One-sigma standard deviation of  $m_{est}^{Bayes}$  for a number of looks  $n = 256$ , in units of  $\text{cm}^3/\text{cm}^3$ . The parameters adopted by the simulation are:  $\sigma_m = 0.005 \text{ cm}^3/\text{cm}^3$ ,  $\sigma_{ks} = 0.01$ ,  $\rho_{\sigma_{vv}^0/\sigma_{vh}^0} = 0.7$  and  $\rho_{\sigma_{vh}^0/\sigma_{vv}^0} = 0.1$ .

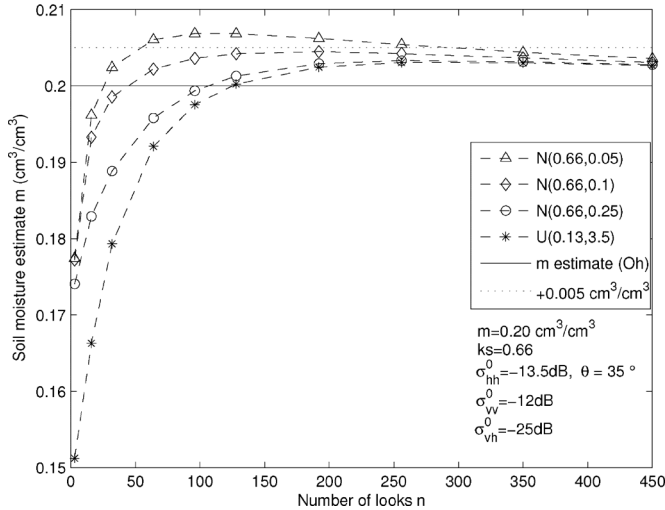


Fig. 6. Bayesian retrievals of soil moisture using Gaussian and uniform distributions as prior information for soil roughness, as a function of the number of looks  $n$ , in units of  $\text{cm}^3/\text{cm}^3$ . Uniform prior  $U(0.04, 0.35)$  is used for soil moisture. The true value from Oh's retrieval is shown along with the  $\sigma_m$ -line, thus indicating the minimum uncertainty that every retrieval might have. The parameters adopted by the simulation are:  $\sigma_m = 0.005 \text{ cm}^3/\text{cm}^3$ ,  $\sigma_{ks} = 0.01$ ,  $\rho_{\sigma_{vv}^0/\sigma_{vh}^0} = 0.7$  and  $\rho_{\sigma_{vh}^0/\sigma_{vv}^0} = 0.1$ .

$N(\mu_{ks}, \sigma'_{ks})$  and we will assess the performance of the retrieval as a function of the number of looks. We start using a  $(\sigma_{hh}^0, \sigma_{vv}^0, \sigma_{vh}^0)$  simulated from  $m = 0.20 \text{ cm}^3/\text{cm}^3$  and  $ks = 0.66$  through the functions  $\sigma_i^0(m, ks)$  ((2)–(4)). In the following paragraph, the behavior of the retrieval when the precision (spread)  $\sigma'_{ks}$  of the prior varies will be analyzed.

Fig. 6 shows the estimated  $m$  for the Bayesian retrieval using uniform and Gaussian distributions as priors for soil roughness, where the latter distributions are centered at the true value  $ks = 0.66$  and the precision takes values of 0.05, 0.1 and 0.25. A uniform prior  $U(0.04, 0.35)$  is used for soil moisture. For the number of looks  $n > 300$ , all the estimates tend to the true value of  $m = 0.20 \text{ cm}^3/\text{cm}^3$  within the  $0.005 \text{ cm}^3/\text{cm}^3$  range, which is the intrinsic heterogeneity of the soil given by  $\sigma_m$ . This true value is also the estimated  $m$  derived from Oh's model ( $m_{est}^{Oh}$ ),

which does not depend on  $n$  since Oh's model does not take into account speckle. As expected, the retrieval schemes weights the likelihood using the prior, and different rates of convergence are reached. However, two regions are readily determined. On one hand, a region for large  $n$ , where it is observed that the retrieval with uniform prior converges faster than when a Gaussian prior is used. On the other hand, a precise prior is preferable for low  $n$  ( $n < 50$ ), where it is observed that  $N(0.66, 0.05)$  approaches to the true  $m = 0.20 \text{ cm}^3/\text{cm}^3$  value faster (i.e., with a higher slope) than an imprecise one ( $N(0.66, 0.25)$ ) and even faster than when a uniform prior  $U(0.13, 3.5)$  is used. In other words, when variance from speckle is significant (low values of  $n$ ), a precise prior improves the retrieval by strongly restricting the possible values of  $m$ , whereas for large  $n$  any prior performs equally well, specially the uniform one. For  $n > 300$ , the error  $m_{std}$  is less than  $0.03 \text{ cm}^3/\text{cm}^3$ , where for  $n < 50$  the error is about  $0.06 - 0.07 \text{ cm}^3/\text{cm}^3$ .

In Fig. 6, a small overestimation of  $m_{est}^{Bayes}$  is observed ( $< 0.005 \text{ cm}^3/\text{cm}^3$ ) for large  $n$  ( $> 350$ ). Further numerical simulations suggest that this bias is related to the choice of the priors. In the particular case of Fig. 6, the roughness priors were normally distributed centered at the true value of  $ks$  whereas a uniform prior for soil moisture was employed. In these cases, the Bayesian retrieval scheme may suggest an overestimation of the true soil moisture values. On the other hand, when a Gaussian assumption for soil moisture is made (results not shown) overestimation as well as underestimation is found for  $m_{est}^{Bayes}$ . In more general cases, where the priors are neither necessary normally distributed nor centered around the true value, a more complex behavior was observed which deserves further analysis.

## V. CONCLUSION

Surface soil moisture estimation from SAR data is a complex task. This is related to many issues, but the spatiotemporal dynamics of soil moisture and the low dynamic ranges of soil backscatter involved are among the most important ones. Solutions to this complex problem should include better and more tested forward and inverse models. However, it is important to understand that inverse models should address in some way the two phenomena that most degrade the retrieval: speckle and soil spatial heterogeneities. In order to address these issues, a Bayesian methodology has been proposed.

In this methodology, a model for the soil backscattering and a model for the speckle are combined using the framework of the multiplicative model and Bayes' theorem. Therefore, this methodology is able to take into account terrain features as well as speckle noise to achieve a robust retrieval of soil parameters from SAR data. This Bayesian methodology: (1) needs only a forward model (as the Bayesian approach itself is the inversion procedure applied to forward model data), (2) gives an estimation of soil parameters as well as their associated error, (3) can include as many error sources as necessary, and (4) can include prior information in a systematic way.

To illustrate the retrieval scheme, a simplified formulation of Oh's model was used throughout this work. Furthermore, the speckle was modeled using appropriate distributions. Using reasonable hypothesis about functions and model parameters, the



retrieval scheme was tested in different scenarios by means of numerical simulations.

For any soil condition, when the number of looks  $n$  is low and uniform priors for soil parameters are used, the retrieval errors are large. However, when significant multilooking ( $n = 256$ ) is present, the retrieval error decreases. The relative improvement due to the increasing of  $n$  is displayed by the one-sigma contour lines, where error decreases from  $\sim 0.07 \text{ cm}^3/\text{cm}^3$  to  $\sim 0.03 \text{ cm}^3/\text{cm}^3$ .

The effect on the retrieval of different prior distributions was also studied. Comparing Gaussian and uniform priors gives rise to two well-defined behavior for the soil moisture estimates in terms of the number of looks  $n$ . For large  $n$  ( $n > 300$ ), both uniform and Gaussian priors work well (i.e., convergence is assured within the intrinsic variance of the soil moisture). For low values of  $n$  ( $n < 50$ ), a precise prior (i.e.,  $\sigma_{ks}^2 = 0.05$ ) determines a rate of convergence higher than an imprecise one (i.e.,  $\sigma_{ks}^2 = 0.25$ ). A small overestimation is observed ( $< 0.005 \text{ cm}^3/\text{cm}^3$ ) for large  $n$  ( $> 350$ ). This bias could be related to the choice of the priors.

In summary, the proposed soil moisture retrieval scheme takes as inputs the measured soil backscattering coefficients, soil ancillary parameters and the number of looks, among others. Soil ancillary parameters are related to the expected distribution of soil parameters within the SAR pixel. So defined, soil moisture estimation converges to the expected behavior when  $\sigma_m \rightarrow 0$ ,  $\sigma_{ks} \rightarrow 0$  and  $n \rightarrow \infty$ , confirming that the standard Oh's model regime is reached.

Due to its conception, the presented model is able to study the performance of different retrieval schemes for different types of soils and/or different soil moisture spatial distributions. Furthermore, since soil variance increases with scale, multilooking will reduce speckle variance but also will increase observed soil parameters variance ( $\sigma_m^2, \sigma_{ks}^2$ ), thus ultimately degrading the retrieval. Therefore, the proposed scheme is a useful tool to investigate, given an error requirement, which is the optimum number of looks for soil moisture retrieval in a given soil condition (degree of heterogeneity).

#### ACKNOWLEDGMENT

The authors would like to thank C. Notarnicola and D. Dadamia for their helpful review comments. The authors also thank the anonymous reviewers for their thoughtful comments for improving the manuscript.

#### REFERENCES

- [1] Y. Kerr, "Soil moisture from space: Where are we?," *Hydrogeol. J.*, vol. 15, no. 10.1007/s10040-006-0095-3, pp. 117–120, 2007.
- [2] F. T. Ulaby, R. K. Moore, and A. K. Fung, *Microwave Remote Sensing: Active and Passive. Radar Remote Sensing and Surface Scattering and Emission Theory*. Boston, MA: Addison-Wesley, 1982, vol. 2.
- [3] C. Oliver and S. Quegan, *Understanding Synthetic Aperture Radar Images*. New York: SciTech Publishing, 2004.
- [4] A. K. Fung, *Microwave Scattering and Emission Models and Their Applications*. Boston, MA: Artech House, 1994.
- [5] A. W. Western, R. B. Grayson, G. Blöschl, G. R. Willgoose, and T. A. McMahon, "Observed spatial organization of soil moisture and its relation to terrain indices," *Water Resources Research*, vol. 35, no. 3, pp. 797–810, 1999.
- [6] N. E. C. Verhoest, H. Lievens, W. Wagner, J. Alvarez-Mozos, M. S. Moran, and F. Mattia, "On the soil roughness parameterization problem in soil moisture retrieval of bare surfaces from synthetic aperture radar," *Sensors*, vol. 8, pp. 4213–4248, Jul. 2008.
- [7] G. Satalino, F. Mattia, M. W. J. Davidson, T. Le Toan, G. Pasquariello, and M. Borgeaud, "On current limits of soil moisture retrieval from ERS-SAR data," *IEEE Trans. Geosci. Remote Sens.*, vol. 40, no. 11, pp. 2438–2447, Nov. 2002.
- [8] J. S. Lee, K. W. Hoppel, S. A. Mango, and A. R. Miller, "Intensity and phase statistics of multilook polarimetric and interferometric SAR imagery," *IEEE Trans. Geosci. Remote Sens.*, vol. 32, no. 5, pp. 1017–1028, Sep. 1994.
- [9] J. S. Lee, J.-H. Wen, T. L. Ainsworth, K.-S. Chen, and A. J. Chen, "Improved sigma filter for speckle filtering of SAR imagery," *IEEE Trans. Geosci. Remote Sens.*, vol. 47, no. 1, pp. 202–213, Jan. 2009.
- [10] C. Lopez-Martinez, I. Hajnsek, J. S. Lee, E. Pottier, and X. Fabregas, "Polarimetric speckle noise effects in quantitative physical parameters retrieval," *IEE Proc. - Radar, Sonar and Navigation*, vol. 153, no. 3, pp. 250–259, Jun. 2006.
- [11] I. Hajnsek, E. Pottier, and S. R. Cloude, "Inversion of surface parameters from polarimetric SAR," *IEEE Trans. Geosci. Remote Sens.*, vol. 41, no. 4, pp. 727–744, Apr. 2003.
- [12] A. Balenzano, F. Mattia, G. Satalino, and M. W. J. Davidson, "Dense temporal series of C- and L-band SAR data for soil moisture retrieval over agricultural crops," *IEEE J. Sel. Topics Appl. Earth Observ. Remote Sens. (JSTARS)*, vol. 4, no. 2, pp. 439–450, Jun. 2011.
- [13] F. Mattia, G. Satalino, V. R. N. Pauwels, and A. Loew, "Soil moisture retrieval through a merging of multi-temporal l-band sar data and hydrologic modelling," *Hydrol. Earth Syst. Sci.*, vol. 13, no. 3, pp. 343–356, 2009.
- [14] Y. Kim and J. J. van Zyl, "A time-series approach to estimate soil moisture using polarimetric radar data," *IEEE Trans. Geosci. Remote Sens.*, vol. 47, no. 8, pp. 2519–2527, Aug. 2009.
- [15] N. E. C. Verhoest, B. De Baets, F. T. Ulaby, G. Satalino, C. Lucau, and P. A. Defourny, "A possibilistic approach to soil moisture retrieval from ERS synthetic aperture radar backscattering under soil roughness uncertainty," *Water Resources Research*, vol. 43, no. 7, p. W07435, 2007.
- [16] H. Vermieuwe, N. E. C. Verhoest, H. Lievens, and B. De Baets, "Possibilistic soil roughness identification for uncertainty reduction on SAR-retrieved soil moisture," *IEEE Trans. Geosci. Remote Sens.*, vol. 49, no. 2, pp. 628–638, Feb. 2011.
- [17] Y. Oh, K. Sarabandi, and F. T. Ulaby, "An empirical model and an inversion technique for radar scattering from bare soil surfaces," *IEEE Trans. Geosci. Remote Sens.*, vol. 30, no. 2, pp. 370–381, Mar. 1992.
- [18] P. C. Dubois, J. van Zyl, and T. Engman, "Measuring soil moisture with imaging radars," *IEEE Trans. Geosci. Remote Sens.*, vol. 33, no. 4, pp. 915–926, Jul. 1995.
- [19] Y. Oh, "Quantitative retrieval of soil moisture content and surface roughness from multipolarized radar observations of bare soil surfaces," *IEEE Trans. Geosci. Remote Sens.*, vol. 42, no. 3, pp. 596–601, Mar. 2004.
- [20] Z. S. Haddad, P. D. Dubois, and J. J. van Zyl, "Bayesian estimation of soil parameters from radar backscatter data," *IEEE Trans. Geosci. Remote Sens.*, vol. 34, no. 1, pp. 76–82, Jan. 1996.
- [21] C. Notarnicola and F. Posa, "Bayesian algorithm for the estimation of the dielectric constant from active and passive remotely sensed data," *IEEE Geosci. Remote Sens. Lett.*, vol. 1, no. 3, pp. 179–183, Jul. 2004.
- [22] F. Mattia, G. Satalino, L. Dente, and G. Pasquariello, "Using a priori information to improve soil moisture retrieval from ENVISAT ASAR AP data in semiarid regions," *IEEE Trans. Geosci. Remote Sens.*, vol. 44, no. 4, pp. 900–912, Apr. 2006.
- [23] S. R. Cloude and E. Pottier, "A review of target decomposition theorems in radar polarimetry," *IEEE Trans. Geosci. Remote Sens.*, vol. 34, no. 2, pp. 498–518, Mar. 1996.
- [24] A. Tarantola, *Inverse Problem Theory and Methods for Model Parameter Estimation*. Philadelphia, PA: Society for Industrial and Applied Mathematics (SIAM), 2005.
- [25] C. R. Vogel, *Computational Methods for Inverse Problems*. Philadelphia, PA, USA: Society for Industrial and Applied Mathematics (SIAM), 2002.
- [26] K. S. Chen, T.-D. Wu, L. Tsang, Q. Li, J. Shi, and A. K. Fung, "Emission of rough surfaces calculated by the integral equation method with comparison to three-dimensional moment method simulations," *IEEE Trans. Geosci. Remote Sens.*, vol. 41, no. 1, pp. 90–101, Jan. 2003.
- [27] A. K. Fung and K. S. Chen, "An update on the IEM surface backscattering model," *IEEE Geosci. Remote Sens. Lett.*, vol. 1, no. 2, pp. 75–77, Apr. 2004.

- [28] K. Song, X. Zhou, and Y. Fan, "Empirically adopted IEM for retrieval of soil moisture from radar backscattering coefficients," *IEEE Trans. Geosci. Remote Sens.*, vol. 47, no. 6, pp. 1662–1672, Jun. 2009.
- [29] A. Merzouki, H. McNairn, and A. Pacheco, "Mapping soil moisture using RADARSAT-2 data and local autocorrelation statistics," *IEEE J. Sel. Topics Appl. Earth Observ. Remote Sens. (JSTARS)*, vol. 4, no. 1, pp. 128–137, Mar. 2011.
- [30] M. Callens, N. E. C. Verhoest, and M. W. J. Davidson, "Parameterization of tillage-induced single-scale soil roughness from 4-m profiles," *IEEE Trans. Geosci. Remote Sens.*, vol. 44, no. 4, pp. 878–888, Mar. 2006.
- [31] D. J. C. MacKay, *Information Theory, Inference, and Learning Algorithms*. Cambridge, UK: Cambridge University Press, 2003.
- [32] A. W. Western and G. Blöschl, "On the spatial scaling of soil moisture," *J. Hydrol.*, vol. 217, no. 3–4, pp. 203–224, 1999.
- [33] T. J. Jackson, H. McNairn, M. A. Weltz, B. Brisco, and R. Brown, "First order surface roughness correction of active microwave observations for estimating soil moisture," *IEEE Trans. Geosci. Remote Sens.*, vol. 35, no. 4, pp. 1065–1069, Jul. 1997.
- [34] L. Wasserman, *All of Statistics: A Concise Course in Statistical Inference*. New York: Springer, 2004.



**Matias Barber** received the degree in physics from the University of Buenos Aires, Argentina, in 2009. He is currently pursuing the Ph.D. degree working on surface scattering models at the Instituto de Astronomía y Física del Espacio (IAFE), Buenos Aires, Argentina. Since 2007 he is also responsible for development of laser profilers and field work.



**Francisco Grings** received the Ph.D. degree in 2008. He is a physicist and a junior research member of Consejo Nacional de Investigaciones Científicas y Técnicas (CONICET) working at Instituto de Astronomía y Física del Espacio (IAFE), Buenos Aires, Argentina. He is responsible for remote sensing modeling within IAFE's remote sensing group. He is leading the Observing System Simulation Experiment (OSSE) project at IAFE.



**Pablo Perna** is a student in computer science finishing his career at the University of Buenos Aires. He is a consultant for Instituto de Astronomía y Física del Espacio (IAFE), Buenos Aires, Argentina, and responsible for computer simulations and data acquisition algorithms.



emphasis on satellite data applications in soil properties.

**Marcela Piscitelli** is an agronomist graduated from the University of Buenos Aires, Argentina, in 1980, and received her Magister degree in Remote Sensing and Geographic Information Systems from the Universidad del Centro (UNCPBA) in 2009. Since 1989 she is Professor of Soil Management and Conservation at UNCPBA. Her research here is focused on soil cartography, soil physical degradation and soil water erosion. She has field experience in soil conservation tillage using experimental plots. Latterly, she focused her research on soil remote sensing with particular



**Martín Maas** is currently pursuing the Licenciatura degree in Applied Mathematics, at the University of Buenos Aires. He works in numerical electromagnetics and statistical modeling in microwave remote sensing, at the Instituto de Astronomía y Física del Espacio (IAFE), Buenos Aires, Argentina.



**Cintia Bruscantini** is an electronic engineer currently pursuing the engineering Ph.D. degree in observing systems simulations at the Instituto de Astronomía y Física del Espacio (IAFE), Buenos Aires, Argentina. She has been working on developing an Observing System Simulation Experiment (OSSE) for the Aquarius soil moisture product. She is also collaborating with the National Commission on Space Activities (CONAE) of Argentina for the calibration of the microwave radiometer (MWR) on board the Aquarius/SAC-D.



**Julio Jacobo-Berlles** received the Eng. degree in electronics and the Ph.D. degree in computer science from the University of Buenos Aires, Buenos Aires, Argentina, in 1983 and 2005, respectively. His current research interests include microwave remote sensing, image processing, and computer vision. He is currently an Adjoint Professor at the Computer Science Department, Faculty of Exact and Natural Sciences, University of Buenos Aires and is currently involved in a collaboration project related to the Argentine SAOCOM SAR mission.



related to applications and quality analysis of the future Argentine SAOCOM SAR mission products.

**Haydee Karszenbaum** is a physicist and research member of Consejo Nacional de Investigaciones Científicas y Técnicas (CONICET), a remote sensing specialist, and Director of the Remote Sensing Group at the Instituto de Astronomía y Física del Espacio (IAFE), Buenos Aires, Argentina. Since 1983, she has worked in remote sensing, and since 1997, she has been dedicated to microwave remote sensing. She is currently the PI of national projects and of Space Agencies AO projects. She is also coordinating a technology transfer project